Genes to Cells

WILEY

ORIGINAL ARTICLE OPEN ACCESS

Attenuation of Oxygen-Induced Neovascularization and Inflammation by Neutralizing VEGFA and/or ANG-2 With an Antibody

Hirokazu Oohashi[1,2] | Toshiro Iwagawa[1] | Hiroto Abe[3] | Chihiro Kawaji[1] | Yuta Inokuchi[1,3] | Tetsuhiro Soeda[3] | Kosuke Saita[1] | Makoto Aihara[4] | Sumiko Watanabe[1,4]

[1]Department of Retinal Biology and Pathology, Graduate School of Medicine, The University of Tokyo, Tokyo, Japan | [2]Graduate School of Pharmaceutical Sciences, Josai International University, Chiba, Japan | [3]Product Research Dept, Chugai Pharmaceutical Co., Ltd., Togane, Kanagawa, Japan | [4]Department of Ophthalmology, Graduate School of Medicine, The University of Tokyo, Tokyo, Japan

Correspondence: Sumiko Watanabe (sumiko@g.ecc.u-tokyo.ac.jp)

Received: 21 January 2026 | **Revised:** 21 January 2026 | **Accepted:** 17 March 2026

Transmitting Editor: Tadashi Yamamoto

ABSTRACT

Neovascularization is a major cause of blindness in various retinal diseases, and inflammation aggravates the pathological and clinical conditions of these diseases. VEGFA or ANG-2 neutralizing antibodies have been used to block pathological neovascularization. In this work, the effects of intraocular administration of neutralizing antibodies against VEGFA, ANG-2, or bispecific to these two factors on pathological findings were examined in the oxygen-induced retinopathy (OIR) mouse model. At both postnatal day (P)17 and P19, anti-VEGFA and -ANG-2 administration suppressed neovascularization, and the bispecific antibody attenuated neovascularization more efficiently. However, oxygen-induced vaso-obliteration was not modified by these antibodies. Numbers of photoreceptor, amacrine, and bipolar cells were reduced in the OIR retina, and the antibodies reversed these changes. Microglia-specific gene expression increased in the OIR retina, and administration of the antibodies reduced the IBA1-positive area in the OIR retina, although these antibodies did not affect *Iba1* gene expression. Labeled VEGFA and ANG-2 were found to be co-localized with microglia, suggesting that VEGFA and ANG-2 affect microglia activation directly. Taken together, neutralizing antibody to VEGFA or ANG-2 attenuated oxygen-induced neovascularization and inflammation, and the bispecific antibody more efficiently suppressed some features than the single antibody to VEGFA or ANG-2.

1 | Introduction

Neovascularization is a major factor in the impairment and loss of vision in the ischemic retinopathies of various retinal diseases. Retinal hypoxia caused by retinal vessel occlusion or capillary non-perfusion in retinopathies initiates the secretion of angiogenic factors, leading to intraocular neovascularization (NV) (Biswal et al. 2014; Eresch et al. 2018). VEGFA is a major pathophysiological angiogenetic factor (Nagy et al. 2007), and neutralizing antibodies to VEGFA have been developed to hamper neovascularization in disorders such as age-related macular degeneration and diabetic retinopathy (DR) (Fleckenstein et al. 2024; Maheshwari et al. 2023; Osaadon et al. 2014). Since VEGFA induces proliferation of vascular endothelial cells, these therapeutic strategies work primarily by suppressing endothelial cell proliferation (Aiello 1997). Angiopoietin 1 (Ang-1) and angiopoietin 2 (Ang-2) are also important angiogenic-regulating factors, and ANG-2 is known to compete at the TIE2 receptor, which is a signal transducer of ANG-1, leading to vessel destabilization by reduction of receptor phosphorylation (Parikh 2017). This process also contributes to neovascularization and vascular inflammation; therefore, ANG-2 is also seen as a target of not only ocular neovascularization therapy, but also in malignancy (Huang et al. 2010; Hussain et al. 2019). Not only neutralizing

antibody against ANG-2, but a bispecific antibody to VEGFA and ANG-2 (hereinafter referred to as "bispecific antibody") has recently been developed, and clinical use of the antibody has been approved (Liberski et al. 2022; Penha et al. 2024).

Oxygen-induced retinopathy (OIR) is a widely used model of pathological neovascularization in the retina of animal models, such as in mice and rats (Liegl et al. 2019). The effects of various reagents, including VEGFA-neutralizing antibodies, were examined, as was their efficiency to suppress neovascularization using this model (Rojo Arias et al. 2020). ANG-2 also participates in the pathology of the OIR model. The OIR model of a genetically modified mouse that overexpresses ANG-2 showed a worse phenotype with enhanced retinal neovascularization, pericyte deficiency, and enhanced expression levels of *Vegfa* and *Angpt1* (Feng et al. 2007). In contrast, the OIR model of *Angpt2* heterozygous knockout mice showed reduced neovascularization and increased avascular zones at postnatal (P)17 (Feng et al. 2009). However, examination of the effects of neutralizing antibody against ANG-2 in the OIR retina has not been reported.

Various pathological phenomena of OIR have been reported, and inflammation including microglial activation is important in the progression of the pathology of OIR (Dai et al. 2025). Activated microglia secrete pro-inflammatory cytokines (IL-1b, IL-6, IL-8, TNF-a), leading to increased inflammation (Kinuthia et al. 2020). In streptozotocin (STZ)-induced DR model mice, we previously found that, though no vessel abnormality was observed at this pathological stage, activation of the microglia was observed in all retinal layers, and administration of anti-VEGFA, -ANG-2, or bispecific antibody reversed the morphological changes of the microglia (Iwagawa et al. 2025), suggesting the involvement of VEGFA and ANG-2 in the initiation of inflammation not by secondary effects of the regulation of neovascularization.

In this work, using the OIR mouse model, the effects of intraocular administration of anti-VEGFA, -ANG-2, and bispecific antibody on neovascularization and other pathological manifestations observed in the OIR retina were examined.

2 | Results

2.1 | Effects of Anti-VEGFA, -ANG-2, or Bispecific Antibodies on Vaso-Obliteration and Neovascularization

OIR was performed as schematically shown in Figure 1A. The anti-VEGFA, -ANG-2, or bispecific antibodies or control IgG was intravitreally injected into OIR mice at P14, and retinas were harvested at P17 or P19. Immunohistochemistry of retinal whole-mounts using anti-CD31 antibody, a vascular endothelial marker, was performed. Both non-perfusion (vaso-obliteration) and neovascularization regions observed in control IgG-injected samples at P17 were decreased at P19 (Figure 1B–D), suggesting that the retina had started to heal from the oxygen induced stresses. Administration of the antibody did not affect the non-perfusion area at both P17 and P19 (Figure 1B–D); however, the antibodies attenuated neovascularization at P17 (Figure 1B–D), and the bispecific antibody suppressed neovascularization most efficiently at P17 (Figure 1C). At P19, intraocular administration of the antibodies tended to suppress neovascularization, but the differences were not significant, except for the bispecific antibody (Figure 1D).

Proliferation of vascular endothelial cells (ECs) was then examined by immunostaining of retinal frozen sections using antibodies against Ki67, proliferation antigen, and CD31. In normal control, CD31-positive cells were barely observed, but several Ki67-positive CD31-positive cells were observed in the EC area on the inner side of the OIR-control IgG retina (Figure 1E,F). Antibody administration attenuated the CD31-positive area (Figure 1E) and Ki67 and CD31 double-positive signals (Figure 1F).

2.2 | Gene Expression Patterns in OIR

To examine the gene expression patterns of the OIR retina and that treated with antibodies to OIR, RNA sequencing (RNAseq) was performed of normal control and OIR retinas at P17 and P19 derived from mice administered control IgG, anti-VEGFA, -ANG-2, or bispecific antibody. The volcano plot displays an overview of DEGs between samples. Significant numbers of genes were upregulated in OIR, but many fewer genes were downregulated at P17 (Figure 2A). A similar tendency was observed at P19. Expression levels of specific genes of interest were then examined. *Vegfa* transcripts were upregulated in the OIR retina, but administration of the antibodies did not affect their expression levels (Figure 2B). *Angpt2* was also upregulated in OIR, and antibody administration mildly suppressed the level; however, no significant difference was observed between any combinations (Figure 2B). *Vcam1* and *Cxcl10* were upregulated at P19, but not at P17, and both were suppressed by the antibodies, especially bispecific antibody (Figure 2C). From the data of *Cxcl10*, it was suspected that immune-related genes were upregulated in OIR, and that antibody administration is effective to normalize the levels. Therefore, *Aif1*, which encodes IBA1 microglia/macrophage marker, was then examined, and the level of *Aif1* was upregulated both at P17 and P19; however, the antibodies did not affect the levels of *Aif1* (Figure 2D). *Pde6a* and *Arr3* are rod and cone specifically expressed genes, respectively, and both levels were downregulated at P19, and administration of the bispecific antibody reversed the levels of *Arr3* (Figure 2E). Taken together, VEGFA and ANG-2 appear to participate in inflammation and proper differentiation or protection of a retinal subset of cells in OIR.

2.3 | Modulation of the Subsets of Retinal Cells in OIR, and the Effects of the Antibodies on This Phenomenon

Previous work also showed a decreased number of a subset of amacrine cells in OIR retinas (Spix et al. 2016). The state of photoreceptor, amacrine, and bipolar cells in the present model was next examined by immunostaining of retinal frozen sections at P17 and P19 of OIR mice and control using antibodies that recognize retinal subset markers, ARR3 for cone cells, AP2α for amacrine cells (Bassett et al. 2012), and CHX10, which marks bipolar cells (Figure 3). The number of ARR3 cone photoreceptors

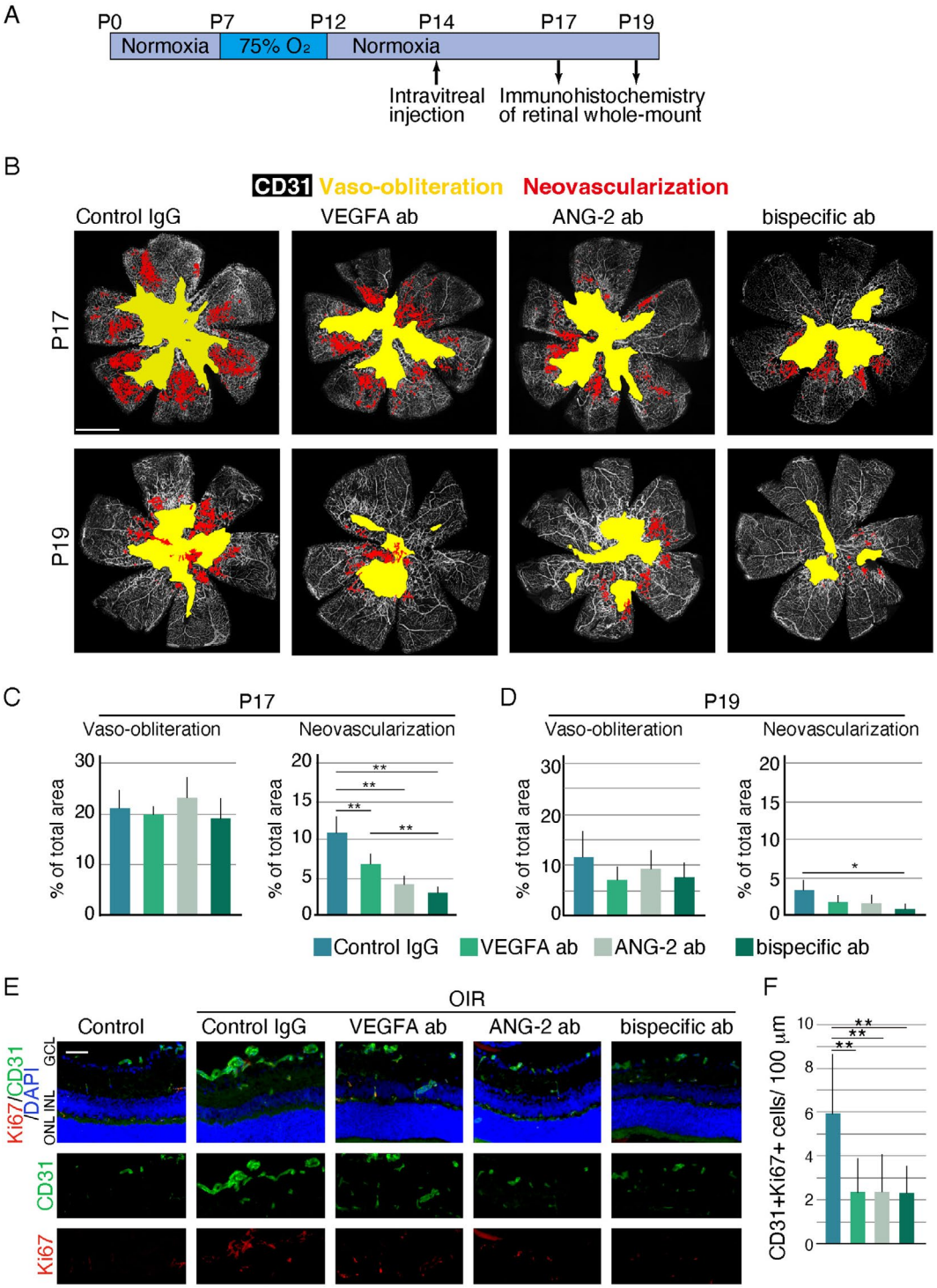

FIGURE 1 | Effects of anti-VEGFA, -ANG-2, or bispecific antibody on pathological neovascularization in the mouse OIR model. (A) Schematic representation of the experimental design to evaluate the effects of intraocular injected antibodies in a mouse OIR model. The antibodies were intravitreally injected into OIR mice at P14. Retinal whole-mounts were prepared at P17 and P19 and immunostained with anti-CD31 antibody. (B) The areas of neovascularization (red) and vaso-obliteration (non-perfusion, yellow) in the OIR retina treated with control IgG, anti-VEGFA antibody, anti-ANG-2 antibody, or anti-VEGFA/ANG-2 bispecific antibody are shown. Scale bar = 1 mm. (C and D) The area (% of total area) of neovascularization and the vaso-obliteration area in the OIR mouse retina. The averages of the area with standard errors are shown in the bar graphs. (E and F) The antibodies were intravitreally injected into OIR mice at P14, and the retina was harvested at P17 and frozen sectioned. Immunostaining with anti-CD31 and -Ki67 antibodies was performed to examine endothelial cell proliferation. Scale bar = 50 μm. Nuclei were visualized with DAPI staining. Numbers of CD31 and Ki67 double-positive cells inner to the INL were counted (F). Data are the averages of 8 samples with standard deviation. (C, D, F) Tukey's HSD test was used for the statistical analysis. *$p < 0.05$; **$p < 0.01$.

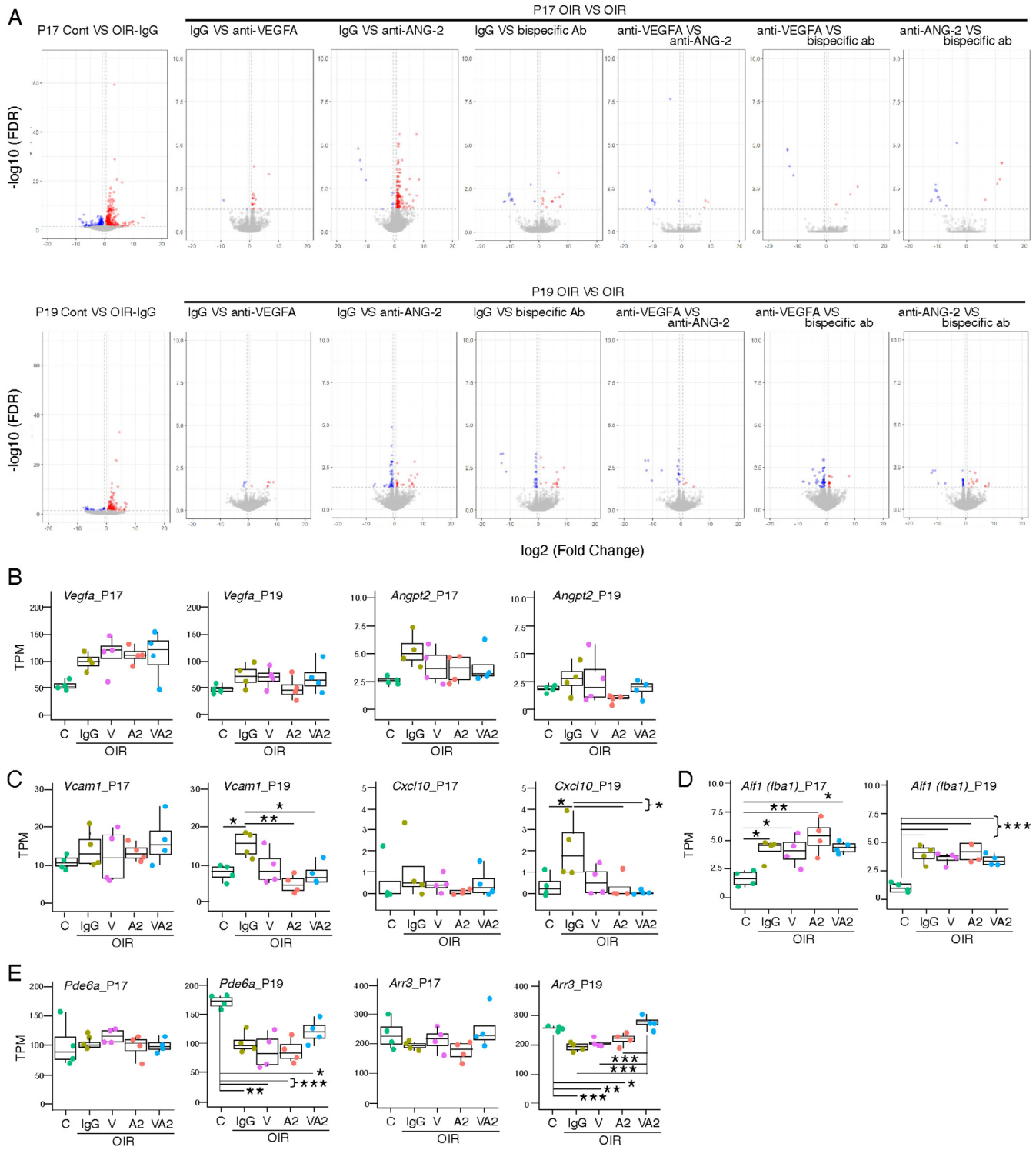

FIGURE 2 | Gene expression patterns of the OIR retina administered antibodies at P17 and P19. RNAseq was performed using whole RNA purified from the retinas of normal mice and OIR mice administered the antibodies. Four samples of each condition were prepared. (A) Volcano plots are shown. Upregulated genes ($\geq \log2\ (1.5)$) are indicated as red circles, and downregulated genes ($\leq -\log2\ (1.5)$) are indicated as blue circles. (B–E) TPM values of specific genes are shown. A2, ANG-2 antibody; C, control; V, VEGFA antibody; VA2, Bispecific antibody. Tukey's HSD test was used for the statistical analysis. $^{*}p < 0.05$; $^{**}p < 0.01$; $^{***}p < 0.001$.

was reduced at both P17 and P19, and administration of the antibodies reversed this phenotype (Figure 3A–C). The bispecific antibody was the most effective to protect cone photoreceptors in OIR (Figure 3C,D). To roughly characterize rod photoreceptors, the thickness of the outer nuclear layer (ONL) was measured. At P17, antibody-administered retinas were slightly thicker than control retinas, and at P19, ONL thickness was reduced by OIR, and administration of anti-ANG-2 or bispecific antibody protected this phenotype (Figure 3D). At both P17 and P19, the number of CHX10-positive cells was decreased compared with the control

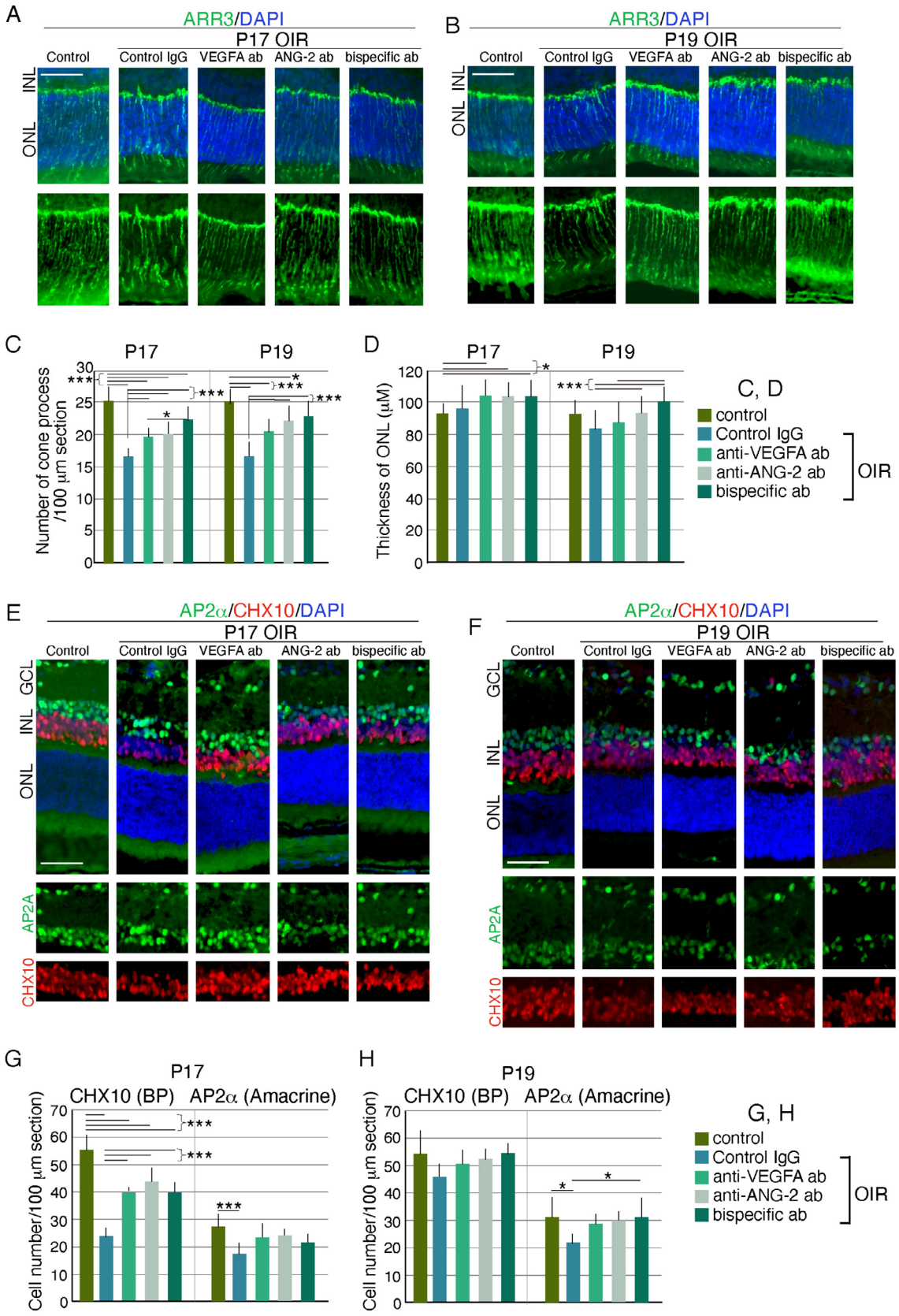

FIGURE 3 | Nature of photoreceptor, amacrine, and bipolar cells and ONL in the OIR retina. The antibodies were intravitreally injected into OIR mice at P14, and the retinas were harvested at P17 or P19 and frozen sectioned. The sections were immunostained with anti-ARR3 (cone), CHX10 (bipolar cells), and AP2α (amacrine) antibodies, and nuclei were visualized with DAPI staining (A, B, E, F). Numbers of ARR3-positive processes are counted (C). ONL thickness at around 100 μm from the optic nerve is measured (D). Numbers of CHX10 or AP2α-positive cells/100-μm section were counted (G, H). Scale bars are 50 μm (A, B, E, F). Data are averages of 8 samples with standard deviation. *$p < 0.05$; ***$p < 0.001$.

(Figure 3E–G), and intraocular administration of the anti-VEGFA, -ANG-2, or bispecific antibody prevented the decrease in the number of CHX10-positive cells at P17 (Figure 3G). A similar tendency was observed at P19 (Figure 3H). The number of AP2α-positive amacrine cells was smaller in the OIR retina than in the control retina at both P17 and P19 (Figure 3E–H). Administration of the antibodies tended to reverse the effects of OIR, but these differences were not significant, except for bispecific antibody at P19 (Figure 3H). To examine whether apoptosis caused the decrease in the number of photoreceptor and INL cells, immunostaining with active CASPASE3 was performed, but no signal was observed at both P17 and P19 (Image data omitted due to space limitations).

GFAP, glial fibrillary acidic protein, is a marker of astrocytes, as well as activated Mueller glial cells. In the control IgG sample, there were strong signals in the basal end of the retinas (Figure S1). No such strong signals were observed in the samples of retinas given anti-VEGFA, ANG-2, or bispecific antibody (Figure S1).

2.4 | VEGFA/ANG-2 Bispecific Antibody to IBA1-Positive Cells in the OIR Mouse Model

Retinal whole-mounts of OIR mice treated with control IgG, VEGFA, ANG-2, or bispecific antibody were immunostained with IBA1 antibody, and IBA1-positive areas were evaluated by ImageJ (Figure 4A,B). IBA1-positive areas of IgG control showed similar values between P17 and P19, but they were reduced by the addition of the antibodies at P19. At P17, ANG-2 antibody reduced the area significantly (Figure 4B). Whether the effects of the VEGFA or ANG-2 antibody on IBA1-positive cells occur by direct regulation of microglia was next evaluated by examining the behavior of fluorescent-labeled VEGFA or ANG-2. Alexa Fluor 488-conjugated VEGFA or ANG-2 was intravitreally injected into OIR mice at P17. One hour after the injection, retinal whole-mounts were immunostained with CD31 and IBA1 antibodies and observed by a confocal microscope. As indicated by white arrows, co-localization of AF488 and IBA1-positive signals was observed in both VEGFA and ANG-2 samples (Figure 4C).

3 | Discussion

In this work, the effects of intraocular injected anti-VEGFA, -ANG-2, and a bispecific antibody on various manifestations observed in the eye of OIR mouse models were examined. In addition to the anti-VEGFA antibody, suppressive effects of anti-ANG-2 and bispecific antibodies on OIR-induced neovascularization and other pathological manifestations were clearly observed. Transcriptome analysis showed regulation of inflammatory-related transcripts by these antibodies.

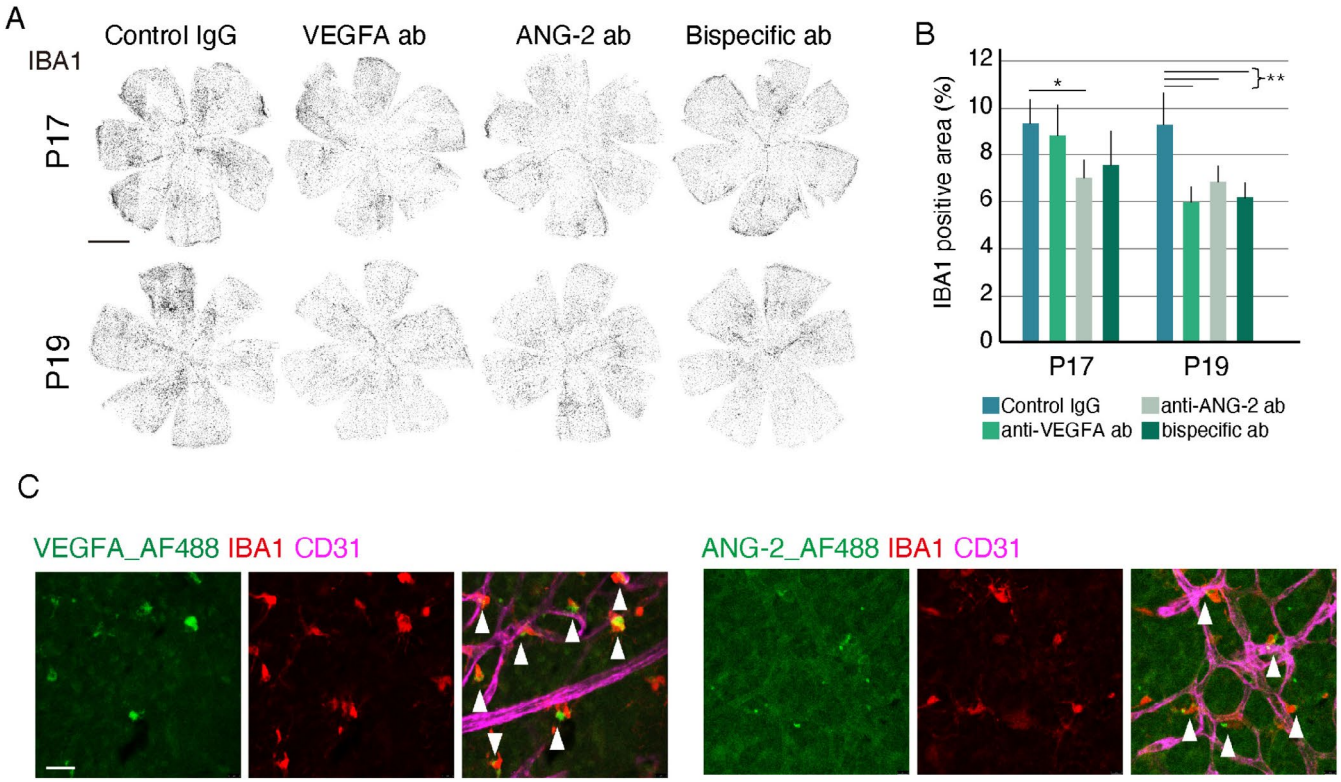

FIGURE 4 | Changes of IBA1-positive cells and the effects of intraocular injected anti-VEGFA, -ANG-2, or bispecific antibody. (A) Retinal whole-mounts of the OIR mice at P17 and P19 treated with control IgG, anti-VEGFA, -ANG-2, or bispecific antibody were immunostained with anti-IBA1 antibody and observed by a confocal microscope. Scale bar = 1 mm. (B) The IBA1 signal-positive area was examined using ImageJ software, and the percentage of the positive area to the whole area is shown in (B). The averages of 3 independent samples with standard deviation are shown. *$p < 0.05$; **$p < 0.01$. (C) Alexa Fluor (AF) 488-conjugated VEGFA or ANG-2 was intravitreally injected into OIR mice at P17. The eyes were harvested one hour after the injection, and whole-mounts were immunostained with anti-CD31 and anti-IBA1 antibodies and observed by a confocal microscope. White arrowheads indicate VEGFA- or ANG-2-Alexa Fluor 488 signals in IBA1-positive cells. Scale bar = 20 μm.

Furthermore, transcriptome analysis indicated protective effects of the antibodies on photoreceptor loss at P19, and this phenomenon is typically observed with bispecific antibody administration. Examination of immunostained sections supported this notion. Previous work demonstrated a photoreceptor decrease by apoptosis in OIR (Gao et al. 2025; Xu et al. 2019). However, apoptosis was not observed by immunohistochemical examination of active CASPASE3 expression in ONL (Image data omitted due to space limitations); therefore, one cannot determine whether the present finding was caused by suppression of apoptosis. Since bispecific antibody was more effective than anti-VEGFA or -ANG-2 antibodies, antibodies against VEGFA or ANG-2 appear to participate in the protection of photoreceptor loss in different ways.

Previous reports showed that dopaminergic amacrine cells decreased, and further analysis showed the presence of active caspase 3 (Cammalleri et al. 2017) of TUNEL-positive cells (Sennlaub et al. 2002) in INL, suggesting that broad apoptosis occurred in INL of OIR. Although active CASPASE 3 signals in INL were not observed in immunostained sections (Image data omitted due to space limitations), decreased numbers of bipolar cells in addition to amacrine cells were clearly observed; furthermore, the suppression of the numbers of both cell types was reversed by the addition of the antibodies. A previous report showed that systemic administration of VEGF-trap protected dopaminergic amacrine in the OIR mouse (Rojo Arias et al. 2020), and the authors suggested that aflibercept supports stabilizing the intraretinal vascular beds, a prerequisite for interneuron nourishment and differentiation (Rojo Arias et al. 2020). Whether the same mechanism can be applied to bipolar cells is currently unknown, but regulation of inflammation by suppressing VEGF and/or ANG-2 is likely at least partly involved in the mechanism.

By transcriptome analysis and whole-mount immunostaining, it was shown that, although suppression of VEGFA and/or ANG-2 did not affect transcript expression of a microglia-specific marker gene, the microglia-occupied area was decreased by antibody administration, suggesting that the administration of the antibodies suppressed inflammation in the OIR retina. Since fluorescent-labeled VEGFA or ANG-2 was observed to be colocalized with the IBA1-positive signal, there may be a direct effect of the antibodies on microglia. In accordance with this notion, previous reports showed that VEGF induced chemotaxis and proliferation of microglial cells (Forstreuter et al. 2002), and ANG-2 can activate microglia through integrin αvβ1 (Li et al. 2020). We previously showed that the antibodies suppressed microglial activation even before neovascularization started in the STZ model (Iwagawa et al. 2025). In this work, the impact of administration of anti-VEGFA, -ANG-2, and bispecific antibodies on various pathological manifestations at P17 and P19 was examined. Significant effects of the antibodies were observed, but the degrees, patterns, and efficacy differed depending on the antibody, as well as the observation stage. The antibody impacts in OIR that were observed may be partly due to the secondary effects of suppression of neovascularization and partly by the direct effects on inflammation-related cells, and these aspects may change at different pathological phases. More detailed time course studies in the early phase of OIR may give information about mechanisms in future work.

4 | Experimental Procedures

4.1 | Mice

All animal experiments were approved by the Institutional Animal Research Committee of the University of Tokyo and were conducted in accordance with the Association for Research in Vision and Ophthalmology Statement for the Use of Animals in Ophthalmic and Vision Research. C57BL/6J wild-type mice were purchased from Japan SLC Inc. (Shizuoka, Japan).

4.2 | OIR Model Mice and Antibody Administration

C57BL/6J mouse pups and their mothers were exposed to 75% O_2 from P7 to P12 and then returned to room air (Liegl et al. 2019). At P14, the OIR mice were anesthetized with isoflurane (FUJIFILM Wako Pure Chemical Corporation, 099-06571) and oxybuprocaine (Santen Pharmaceutical Co. Ltd., 871313), and 1 μL of control IgG (0.4 μg/μL), anti-VEGFA (B20.4.1., 0.2 μg/μL), ANG-2 (LC10, 0.2 μg/μL), or VEGFA/ANG-2 bispecific antibody (B20.4.1_LC10, 0.4 μg/μL), provided by F. Hoffmann-La Roche Ltd. (Basel, Switzerland) was intravitreally injected into the mice.

4.3 | Immunohistochemistry

Immunostaining of retinal frozen sections was performed as previously described (Iwagawa et al. 2025). The primary antibodies used were anti-ARR3 (Millipore, AB15282), AP2α (DSHB, 3B5-s), CHX10 (Exalpha, X1190P164), and GFAP (Sigma-Aldrich, G3893) antibodies. Retinal whole-mounts were prepared and incubated with blocking solution (10% FBS and 0.2% Triton X-100 in PBS) for 1 h at room temperature, then incubated with blocking solution containing rat anti-CD31 antibody (BioLegend, 102501) or rabbit anti-IBA1 antibody (FUJIFILM Wako Pure Chemical Corporation, 018-28523) overnight at 4°C, and incubated with blocking solution containing appropriate secondary antibodies conjugated with Alexa Fluor 488 or 546 (Thermo Fisher Scientific) for 30 min at room temperature. Fluorescence images were obtained using the TCS SP8 confocal microscope (Leica Microsystems) and LAS X software (Leica Microsystems). A fully automated pipeline (http://oirseg.org/) was used to judge and quantify the neovascularization and vaso-obliteration area in the retinal area (Xiao et al. 2017). ImageJ software (https://imagej.nih.gov/ij/; National Institutes of Health, Bethesda, MD, USA) was used to quantify the IBA1-positive area in the retinal area.

5 | RNA Sequencing Analysis

Eyes were enucleated from the sacrificed control and OIR mice at P17 and P19, and the whole retinas were collected using dissecting forceps. One whole retina was used for total RNA extraction using Sepasol-RNA I Super G (Nacalai Tesque, 09379), and 4 independent samples were prepared for one condition. RNA-seq was conducted by Takara Bio Inc. (Shiga, Japan). Briefly, library generation was done using SMART-Seq mRNA

(Takara Bio Inc.), IDT for Illumina—DNA/RNA UD Indexes, Tagmentation (Illumina Inc., San Diego, CA, USA), and Nextera XT DNA Library Prep Kit (Illumina). Library samples were then sequenced with the NovaSeq6000 system (Illumina). Reads were mapped to the mouse genome with RefSeq (GRCm38.p4) transcript annotation using STAR v2.7.10a (https://github.com/alexdobin/STAR). TPM (transcripts per million) values were calculated using RSEM v1.3.3 (https://github.com/deweylab/RSEM). Differentially expressed genes (DEGs) were identified from read counts using the R package edgeR (version 4.6.1) (Robinson et al. 2010). Genes were considered significantly differentially expressed if they had a false discovery rate (FDR) <0.05 and log2 (fold change) $\geq$ log2 (1.5) for upregulated genes or FDR <0.05 and log2 (fold change) $\leq -$log2 (1.5) for downregulated genes. TPM values of representative genes were considered significantly different by Tukey's HSD test in R (The R Foundation for Statistical Computing, Vienna, Austria); all analyses were performed using R version 4.5.0. Nucleotide sequence data reported are available in the NCBI_GEO databases under the accession numbers GSE315511.

5.1 | In Vivo Injection of Labeled VEGFA or ANG-2 Into OIR Mice

Recombinant VEGFA (Thermo Fisher Scientific, 450-32) and ANG-2 (R&D SYSTEMS, 7186-AN-025) were labeled with Alexa Fluor 488 using a Microscale Protein Labeling Kit (Thermo Fisher Scientific, A30006). OIR mice at P17 were anesthetized with isoflurane and oxybuprocaine, and Alexa Fluor 488-labeled VEGFA or ANG-2 was intravitreally injected into the OIR mice. One hour after injection, the eyes were enucleated and immunostained with anti-IBA1 antibody as described above.

5.2 | Statistical Analysis

p values were calculated by Tukey's HSD test using R software.

Author Contributions

Hirokazu Oohashi: conceptualization, investigation. **Toshiro Iwagawa:** conceptualization, investigation. **Hiroto Abe:** conceptualization, investigation, validation, data curation. **Chihiro Kawaji:** conceptualization, investigation. **Yuta Inokuchi:** conceptualization, investigation, validation, methodology. **Tetsuhiro Soeda:** resources, supervision. **Kosuke Saita:** conceptualization, investigation. **Makoto Aihara:** supervision, resources. **Sumiko Watanabe:** conceptualization, investigation, writing – review and editing, project administration, supervision, data curation.

Acknowledgments

This work is supported by Chugai Pharmaceutical Co. Ltd.

Funding

This work was supported by Chugai Pharmaceutical Co. Ltd.

Ethics Statement

All animal experiments were approved by the Animal Care Committee of the University of Tokyo hospital, University of Tokyo and were conducted in accordance with the Association for Research in Vision and Ophthalmology (ARVO) statement for the use of animals in ophthalmic and vision research.

Conflicts of Interest

The authors declare no conflicts of interest.

Data Availability Statement

The data that support the findings of this study are available from the corresponding author upon reasonable request.

References

Aiello, L. P. 1997. "Vascular Endothelial Growth Factor. 20th-Century Mechanisms, 21st-Century Therapies." *Investigative Ophthalmology and Visual Science* 38: 1647–1652.

Bassett, E. A., A. Korol, P. A. Deschamps, et al. 2012. "Overlapping Expression Patterns and Redundant Roles for AP-2 Transcription Factors in the Developing Mammalian Retina." *Developmental Dynamics* 241: 814–829. https://doi.org/10.1002/dvdy.23762.

Biswal, M. R., H. M. Prentice, C. K. Dorey, and J. C. Blanks. 2014. "A Hypoxia-Responsive Glial Cell-Specific Gene Therapy Vector for Targeting Retinal Neovascularization." *Investigative Ophthalmology & Visual Science* 55: 8044–8053. https://doi.org/10.1167/iovs.14-13932.

Cammalleri, M., F. Locri, E. Catalani, et al. 2017. "The Beta Adrenergic Receptor Blocker Propranolol Counteracts Retinal Dysfunction in a Mouse Model of Oxygen Induced Retinopathy: Restoring the Balance Between Apoptosis and Autophagy." *Frontiers in Cellular Neuroscience* 11: 395. https://doi.org/10.3389/fncel.2017.00395.

Dai, Q., W. Su, Z. Zhou, et al. 2025. "DDR2 Alleviates Retinal Vaso-Obliteration and Pathological Neovascularization by Modulating Microglia M1/M2 Phenotypic Polarization in a Mouse Model of Proliferative Retinopathy." *Biochimica et Biophysica Acta, Molecular Basis of Disease* 1871: 167787. https://doi.org/10.1016/j.bbadis.2025.167787.

Eresch, J., M. Stumpf, A. Koch, et al. 2018. "Sphingosine Kinase 2 Modulates Retinal Neovascularization in the Mouse Model of Oxygen-Induced Retinopathy." *Investigative Ophthalmology & Visual Science* 59: 653–661. https://doi.org/10.1167/iovs.17-22544.

Feng, Y., F. vom Hagen, F. Pfister, et al. 2007. "Impaired Pericyte Recruitment and Abnormal Retinal Angiogenesis as a Result of Angiopoietin-2 Overexpression." *Thrombosis and Haemostasis* 97: 99–108.

Feng, Y., Y. Wang, F. Pfister, J.-L. Hillebrands, U. Deutsch, and H.-P. Hammes. 2009. "Decreased Hypoxia-Induced Neovascularization in Angiopoietin-2 Heterozygous Knockout Mouse Through Reduced MMP Activity." *Cellular Physiology and Biochemistry* 23: 277–284. https://doi.org/10.1159/000218174.

Fleckenstein, M., S. Schmitz-Valckenberg, and U. Chakravarthy. 2024. "Age-Related Macular Degeneration: A Review." *JAMA* 331: 147–157. https://doi.org/10.1001/jama.2023.26074.

Forstreuter, F., R. Lucius, and R. Mentlein. 2002. "Vascular Endothelial Growth Factor Induces Chemotaxis and Proliferation of Microglial Cells." *Journal of Neuroimmunology* 132: 93–98. https://doi.org/10.1016/s0165-5728(02)00315-6.

Gao, S., S. Gao, Y. Wang, et al. 2025. "Inhibition of Vascular Endothelial Growth Factor Reduces Photoreceptor Death in Retinal Neovascular Disease via Neurotrophic Modulation in Müller Glia." *Molecular Neurobiology* 62: 6352–6368. https://doi.org/10.1007/s12035-025-04689-9.

Huang, H., A. Bhat, G. Woodnutt, and R. Lappe. 2010. "Targeting the ANGPT-TIE2 Pathway in Malignancy." *Nature Reviews. Cancer* 10: 575–585. https://doi.org/10.1038/nrc2894.

Hussain, R. M., A. E. Neiweem, V. Kansara, A. Harris, and T. A. Ciulla. 2019. "Tie-2/Angiopoietin Pathway Modulation as a Therapeutic Strategy for Retinal Disease." *Expert Opinion on Investigational Drugs* 28: 861–869. https://doi.org/10.1080/13543784.2019.1667333.

Iwagawa, T., Y. Inokuchi, K. Saita, et al. 2025. "Effects of VEGFA and ANGPT2 Antibodies on the Activation of Microglia in the Early Stages of Streptozotocin-Induced Pathogenesis of Diabetic Retinopathy." *Genes to Cells* 30: e70036. https://doi.org/10.1111/gtc.70036.

Kinuthia, U. M., A. Wolf, and T. Langmann. 2020. "Microglia and Inflammatory Responses in Diabetic Retinopathy." *Frontiers in Immunology* 11: 564077. https://doi.org/10.3389/fimmu.2020.564077.

Li, Z., E. A. Korhonen, A. Merlini, et al. 2020. "Angiopoietin-2 Blockade Ameliorates Autoimmune Neuroinflammation by Inhibiting Leukocyte Recruitment Into the CNS." *Journal of Clinical Investigation* 130: 1977–1990. https://doi.org/10.1172/JCI130308.

Liberski, S., M. Wichrowska, and J. Kocięcki. 2022. "Aflibercept Versus Faricimab in the Treatment of Neovascular Age-Related Macular Degeneration and Diabetic Macular Edema: A Review." *International Journal of Molecular Sciences* 23: 9424. https://doi.org/10.3390/ijms23169424.

Liegl, R., C. Priglinger, and A. Ohlmann. 2019. "Induction and Readout of Oxygen-Induced Retinopathy." *Methods in Molecular Biology* 1834: 179–191. https://doi.org/10.1007/978-1-4939-8669-9_13.

Maheshwari, S. Y., S. Kumar, A. H. Sinha, and M. Kumar. 2023. "Diabetic Retinopathy: A Pharmacological Consideration." *Cureus* 15: e46842. https://doi.org/10.7759/cureus.46842.

Nagy, J. A., A. M. Dvorak, and H. F. Dvorak. 2007. "VEGF-A and the Induction of Pathological Angiogenesis." *Annual Review of Pathology* 2: 251–275. https://doi.org/10.1146/annurev.pathol.2.010506.134925.

Osaadon, P., X. J. Fagan, T. Lifshitz, and J. Levy. 2014. "A Review of Anti-VEGF Agents for Proliferative Diabetic Retinopathy." *Eye* 28: 510–520. https://doi.org/10.1038/eye.2014.13.

Parikh, S. M. 2017. "Angiopoietins and Tie2 in Vascular Inflammation." *Current Opinion in Hematology* 24: 432–438. https://doi.org/10.1097/MOH.0000000000000361.

Penha, F. M., M. Masud, Z. A. Khanani, et al. 2024. "Review of Real-World Evidence of Dual Inhibition of VEGF-A and ANG-2 With Faricimab in NAMD and DME." *International Journal of Retina and Vitreous* 10: 5. https://doi.org/10.1186/s40942-024-00525-9.

Robinson, M. D., D. J. McCarthy, and G. K. Smyth. 2010. "edgeR: A Bioconductor Package for Differential Expression Analysis of Digital Gene Expression Data." *Bioinformatics* 26: 139–140. https://doi.org/10.1093/bioinformatics/btp616.

Rojo Arias, J. E., M. Economopoulou, D. A. Juárez López, et al. 2020. "VEGF-Trap Is a Potent Modulator of Vasoregenerative Responses and Protects Dopaminergic Amacrine Network Integrity in Degenerative Ischemic Neovascular Retinopathy." *Journal of Neurochemistry* 153: 390–412. https://doi.org/10.1111/jnc.14875.

Sennlaub, F., Y. Courtois, and O. Goureau. 2002. "Inducible Nitric Oxide Synthase Mediates Retinal Apoptosis in Ischemic Proliferative Retinopathy." *Journal of Neuroscience: The Official Journal of the Society for Neuroscience* 22: 3987–3993. https://doi.org/10.1523/JNEUROSCI.22-10-03987.2002.

Spix, N. J., L.-L. Liu, Z. Zhang, et al. 2016. "Vulnerability of Dopaminergic Amacrine Cells to Chronic Ischemia in a Mouse Model of Oxygen-Induced Retinopathy." *Investigative Ophthalmology and Visual Science* 57: 3047–3057. https://doi.org/10.1167/iovs.16-19346.

Xiao, S., F. Bucher, Y. Wu, et al. 2017. "Fully Automated, Deep Learning Segmentation of Oxygen-Induced Retinopathy Images." *JCI Insight* 2: e97585. https://doi.org/10.1172/jci.insight.97585.

Xu, W., Y. Wu, Z. Hu, et al. 2019. "Exosomes From Microglia Attenuate Photoreceptor Injury and Neovascularization in an Animal Model of Retinopathy of Prematurity." *Molecular Therapy–Nucleic Acids* 16: 778–790. https://doi.org/10.1016/j.omtn.2019.04.029.

Supporting Information

Additional supporting information can be found online in the Supporting Information section. **Figure S1:** Effects of VEGFA, ANG-2, or bispecific antibody on astrocytes in the retina of the OIR mouse was examined. Frozen sections at P17 were immunostained with anti-GFAP antibody, and nuclei were visualized with DAPI staining. Scale bar = 50 μm.